SECOND EUROPEAN CONFERENCE ON EARTHQUAKE ENGINEERING
AND SEISMOLOGY, ISTANBUL AUG. 25-29, 2014

ON THE SELECTION AND SCALING OF GROUND MOTIONS FOR FRAGILITY ANALYSIS OF STRUCTURES

Ioannis P. CHRISTOVASILIS[1], Gian Paolo CIMELLARO[2],
Simone BARANI[3] and Sebastiano FOTI[4]

ABSTRACT

The ground motion selection approach adopted for conducting fragility analysis of structures through nonlinear dynamic analysis can affect significantly the results obtained. The scaling method of the selected ground motions is a second factor that plays a major role as well. This work presents a methodology for the selection and scaling of ground motion time histories in fragility analysis that is based on a combination of existing studies with the introduction of novel steps that are recommended so as to achieve specific objectives. The proposed methodology uses the conditional mean spectra, which are defined for the specific site and the specific structure under examination and for different levels of seismic intensity. Sets of unscaled ground motions are selected to match the mean and variance of the spectral ordinates related to each seismic intensity and the fragility analysis is conducted by scaling each set within predefined limits. To demonstrate the procedure, an application example is presented where the suggested methodology is implemented for a hypothetical five-storey light-frame wood building situated at a specific site in Tuscany, Italy. The results of different fragility analyses are then compared with the results obtained by using the state-of-practice approach of a single set of ground motions scaled uniformly within the context of incremental dynamic analysis procedure.

INTRODUCTION

The ground motion selection and scaling methods adopted for conducting fragility analysis of structures through nonlinear dynamic analysis are two important factors that can significantly affect the results obtained. Incremental dynamic analysis (IDA) (Vamvatsikos and Cornell, 2002) with a general set of ground motions (one that is not related to a specific site) is the current state-of-practice approach for performing fragility analysis and more often for evaluating the collapse fragility curve of a building with respect to the spectral acceleration at its fundamental period (FEMA P695, 2009; Christovasilis et al. 2009b).

Ground motion record selection and scaling techniques are still evolving and there is still debate as to which method is the most appropriate. In most of the approaches with few exceptions (Naeim et al.,

[1] Structural and Earthquake Engineer, dedaLEGNO, Florence, Italy, e-mail: ipc@dedalegno.com
[2] Assistant Professor, Department of Structural, Geotechnical & Building Engineering (DISEG), Politecnico di Torino, Turin, Italy, e-mail: gianpaolo.cimellaro@polito.it
[3] Postdoctoral Research Associate, Dipartimento di Scienze della Terra dell'Ambiente e della Vita (DISTAV), University of Genova, Genova, Italy, e-mail: barani@dipteris.unige.it
[4] Associate Professor, Department of Structural, Geotechnical & Building Engineering (DISEG), Politecnico di Torino, Turin, Italy, e-mail: sebastiano.foti@polito.it

2004), the processes of selecting earthquake ground motions and their scaling to match the design spectrum are separate and distinct. In other words, first one or more time histories are selected, and then appropriate scaling mechanisms for spectrum matching are applied. Several methods of scaling time histories have been proposed in the past. Two basic options can be considered: (i) scaling the spectral ordinate without altering the spectral shape but only the amplitude of the recorded ground motions (Kircher 1993, Naeim and Bhatia 2000) or (ii) scaling the spectral ordinate in the frequency domain modifying the frequency content of the recorded ground motions to obtain a spectral match (Gasparini and Vanmarcke 1976, Silva and Lee 1987, Bolt and Gregor 1993, Department of the Army 2000, Carballo and Cornell 2000). To the second group belong also the scaling methods that use wavelets in the time domain to modify the spectral shape and match the target spectrum (NIST 2011; Heo et al. 2011; Hancock et al. 2008).

Some authors suggest to develop fragility curves on the basis of scaled seismic ground-acceleration records (Grigoriu, 2011), which is obviously in contradiction with the approach proposed by Baker (2011) and FEMAP695. In particular Grigoriu (2011) has provided strong evidence against current procedures that assess the seismic performance of structural systems by fragilities calculated from scaled ground-acceleration records.

The current paper stands in between these two approaches with an attempt to limit the effect of scaling in the development of fragility curves.

In the paper it is presented an innovative procedure for ground motion selection and scaling to develop acceleration time history suites corresponding to each of the ground motion intensity levels selected. After selecting spectrum compatible ground motions for the respective intensity levels, each record of the dataset has been scaled such that the average value of the SRSS spectra does not fall below or above 1.5 times the 5%-damped Conditional Mean spectrum for the GM intensity levels for periods between 0.2T–1.5T sec (where T is the fundamental period of the building).

PROPOSED METHODOLOGY

The methodology for the selection and scaling of ground motion time histories to be used for fragility analysis is based on the following steps:

1. Obtain ground shaking intensities on rock (e.g., from the National Institute of Geophysics and Volcanology (INGV) website http://esse1.mi.ingv.it/d14.html for applications within the Italian territory) and ground-motion deaggregation data (Spallarossa and Barani, 2007; Barani et al., 2009) for probability of exceedance of 2%, 5%, 10% and 22% in 50 years at the natural period of the building of interest ;
2. According to Baker (2011), define the Conditional Mean Spectra (CMS) – mean and standard deviation – by using a Ground Motion Prediction Equation (GMPE) (e.g., Ambraseys et al., 1996) and the correlation coefficients derived by Cimellaro (2013) for European earthquakes;
3. Select suites of unscaled ground motions for each intensity level according to Jayaram et al. (2011);
4. Evaluate site response to derive the design ground motions for the specific site; and
5. Define scaling factors for each suite of ground motions for incremental dynamic analysis (IDA).

The CMS is considered as target spectrum instead of the Uniform Hazard spectrum (UHS) because the selection of ground motions that match the UHS may be too conservative as it implies that large-amplitude spectral values will occur at all periods within a single ground motion (Baker, 2011). Indeed, a UHS accounts for the contribution of different earthquake (EQ) scenarios contributing differently at different spectral periods. The CMS, instead, is based on the prevailing (or mean) EQ scenario at a given period and has a spectral shape that is more realistic since it is based on the spectra of ground motions from a similar EQ scenario. The proposed methodology can be grouped as a *Multi Stripe Analysis* (MSA) because it allows engineers to use different suites of ground motions at different intensity levels. Furthermore, the proposed *Advanced Multi Stripe Analysis* (AMSA) allows taking into account the different frequency contents of low and high intensity motions. Compared to

Single Stripe Analysis (SSA) methods such as in FEMA P695 (2009), the scale factors are maintained within a predefined range.

As the seismic hazard is evaluated with a probabilistic approach based on the assumption of rigid outcrop, the selected ground motions do not account for seismic ground response, which has to be specifically taken into account with reference to ground conditions at the site (step 4). The analysis can be conducted with equivalent linear elastic approaches (Idriss and Seed, 1968) for most ground conditions. Non-linear approaches are necessary in presence of highly deformable or unstable soils (e.g. sites which are likely to develop high water pressures), in which the equivalent linear analysis may be not conservative. In any case, a full characterization of ground conditions is necessary with a measurement on site of the shear wave velocity profile and in the lab of the dynamic response of the soil over a wide range of cyclic shear strains.

APPLICATION EXAMPLE

GROUND MOTION SELECTION

The proposed method has been applied for a hypothetical five-storey light-frame wood building situated at the city of Sanspolcro in Tuscany, Italy. No ground response analysis was performed for this site, assuming that the structure is directly founded on a rigid outcrop. The structure was designed for the 10% probability of exceedance (POE) in 50 years. For this mean return period (MRP), the UHS presents a spectral ordinate of 0.14 g at a period of 1 second, which is the fundamental period of the building. Figure 1 shows the contribution of different earthquake scenarios to the 1s-spectral acceleration corresponding to a 10% POE in 50 years and the comparison between the UHS and the spectrum derived from the GMPE of Ambraseys et al. (1996) for an EQ of magnitude M = 5.75, at a distance R = 15.6 km and an epsilon value of 1.15, where epsilon indicates number of standard deviations by which the (logarithmic) ground motion generated by that M-R pair deviates from the median value estimated by the prediction equation used.

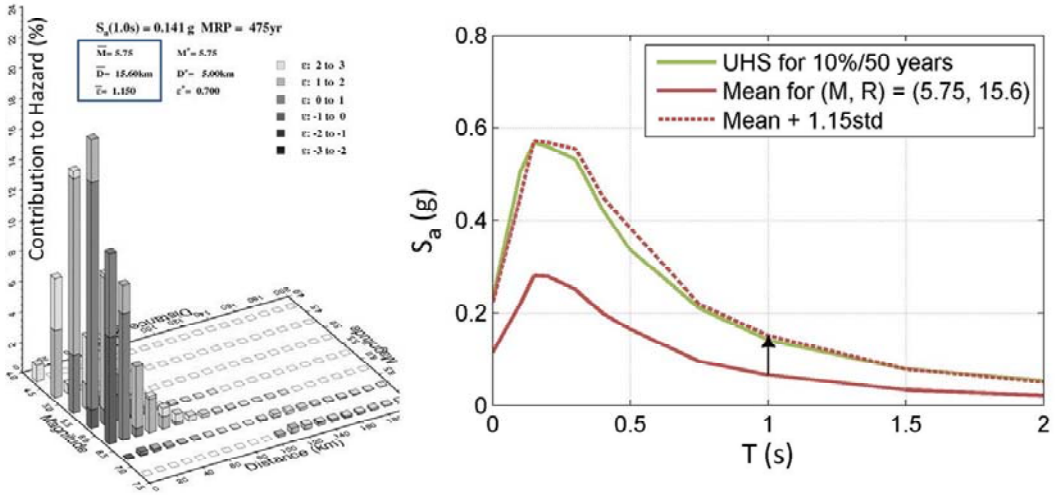

Figure 1. Contributions to the 1s hazard and UHS corresponding to a 10% POE in 50 years for the site of Sansepolcro

Twenty-two pairs of unscaled ground motions were selected for each level of seismic intensity, following the selection algorithm proposed by Jayaram et al. (2011), to match the mean and standard deviation spectral ordinates defined within the context of the CMS procedure. This selection algorithm uses a probabilistic approach to generate multiple response spectra from a target distribution and then selects recorded ground motions whose response spectra individually match the simulated response spectra. The set of selected ground motions is further refined with a greedy optimization technique that improves the match between the target and the sample means and variances.

Figure 2 illustrates the target and achieved mean and standard deviation spectral ordinates, as well as the response spectra of the 22 pairs, in terms of the geometric mean spectrum of the two horizontal components. The UHS is also shown for comparison purposes with the CMS. It can be observed that although the ground motions are unscaled, the procedure of Jayaram et al. (2011) achieves a very good matching of the mean and variance spectral values at all periods. Obviously, the achieved variance in the region of the fundamental period is nonzero, as opposed to the zero target variance, which is a direct effect of the use of unscaled recordings. The selected sets of ground motions were then scaled in order to perform the fragility analysis with specific scale factors, as listed in Table 1, that lie within a predefined range. The resulting mean spectra of the scaled sets are shown in Figure 3. Each record of the dataset has been scaled such that the average value of the SRSS spectra does not fall below or above 1.5 times the 5%-damped Conditional Mean spectrum for the GM intensity levels for periods between 0.2T–1.5T sec (where T is the fundamental period of the building).

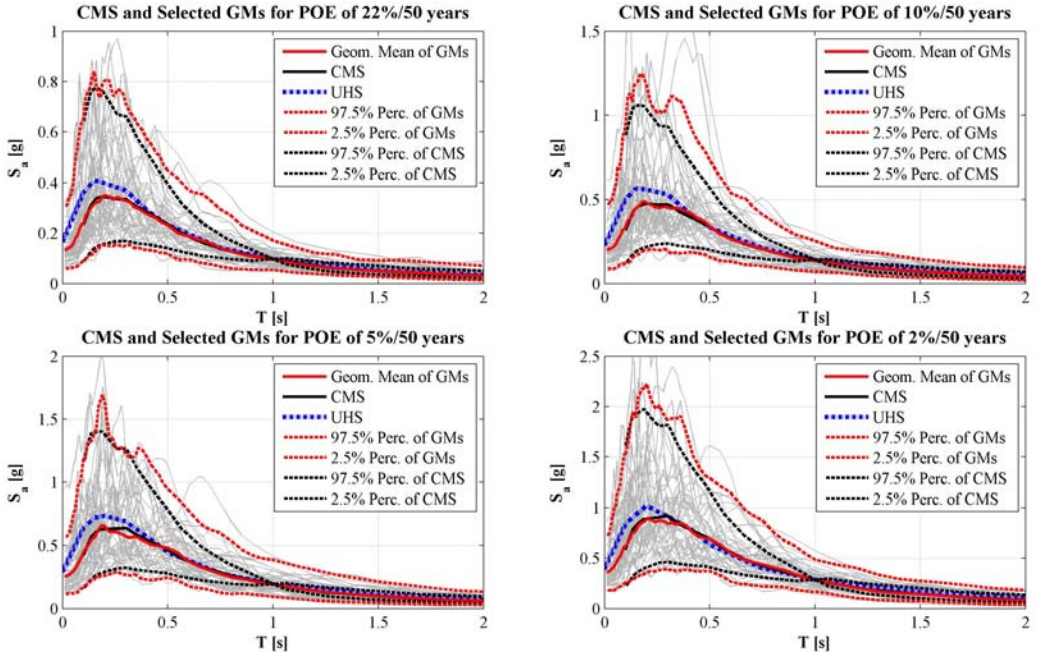

Figure 2. Comparison between target and achieved mean and standard deviation of spectral ordinates of selected ground motions for POE of 22%, 10%. 5% and 2% in 50 years

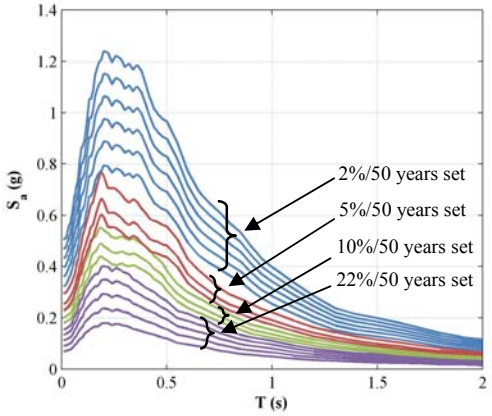

Figure 3. Acceleration response spectra of the ground motion sets as scaled according to Table 1

Table 1. Scale factors used for the IDAs of the AMSA procedure

GM Intensity Level	Scale Factor	Sa (T=1sec) [g]
22% in 50 years	0.513	0.050
	0.676	0.066
	0.838	0.082
	1.000	**0.097**
	1.149	0.112
10% in 50 years	0.897	0.126
	1.000	**0.141**
	1.129	0.159
5% in 50 years	0.907	0.177
	1.000	**0.195**
	1.156	0.226
2% in 50 years	0.894	0.256
	1.000	**0.286**
	1.099	0.315
	1.198	0.343
	1.297	0.372
	1.397	0.400

SEISMIC DESIGN OF THE BUILDING

The structure considered for the application example is a 5-storey residential light-frame wood building with a foot print of 14×10 m. The light-frame wood shear walls that serve as the lateral-load-resisting system are located at the external sides of the structure. The building has been designed for a seismic excitation along its longest side equal to the 10% POE in 50 years and with a behaviour factor q = 3. Figure 4 illustrates the panel configuration of the external side of the building, which is identical for all storeys. Only the full-height panels were considered as lateral-resistant elements for the seismic design. The permanent and accidental loads considered in the design were equal to 3.0 and 0.6 kPa, respectively, for the first 4 storeys. The roof was assumed to have a permanent load of 1.5 kPa and no accidental load in the seismic combination. The total base shear was equal to 53.0 kN. The light-frame wood shear walls consisted of a wood framing of Douglas-Fir with dimensions of 6×16cm, a structural OSB panel with thickness equal to 15 mm and ring nails 2.8 mm in diameter and 65 mm in length. The design resistance of the sheathing-to-framing connection was equal to 0.7 kN. The design procedure yielded an edge nailing of 10 cm for the first two storeys and of 15 cm for the other three storeys above.

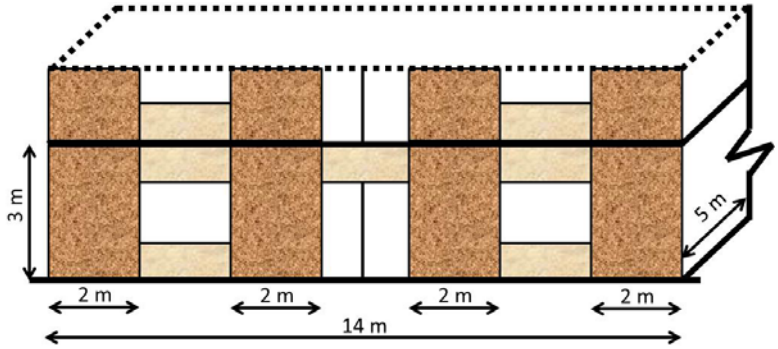

Figure 4. Panel configuration and basic dimensions of the external side of one typical story level of the building

NUMERICAL MODELLING OF THE BUILDING

The numerical modelling and the nonlinear dynamic analyses were conducted using the computer program SAWS: Seismic Analysis of Woodframe Structures, developed within the CUREE-Caltech Woodframe Project by Folz and Filiatrault (2004a; 2004b). This model is based on the so-called "pancake modelling" that considers floor diaphragms to be rigid bodies that translate and rotate in the horizontal plane, conducting thus a degenerated two-dimensional planar analysis for actual three-dimensional structures, as shown in Figure 5c,d. Since the structure was analyzed along a single horizontal direction, the floor diaphragms were constrained to translate only in the direction of the input motion. The source code of SAWS was also modified to include the consideration of first order P-Δ effects. In the SAWS model, each resisting shear wall is modelled by an equivalent nonlinear shear spring element which includes pinching, as well as stiffness and strength degradation, and is governed by 10 different physically identifiable parameters (Folz and Filiatrault 2004a, b). The pinched, strength and stiffness degrading hysteretic behavior of each wood shear wall in the building is characterized using CASHEW, an associated numerical model (Folz and Filiatrault, 2001) that predicts the load-displacement response of the full wall assemblies under general quasi-static cyclic loading, based on sheathing-to-framing connection cyclic test data, and extracts the optimum values of the 10 parameters of a single hysteretic spring, as shown in Figure 5a,b. The sheathing-to-framing parameters used in the wall model were obtained from Christovasilis et al. (2009a).

FRAGILITY ANALYSIS RESULTS

The numerical model described in the previous section was used to perform nonlinear dynamic analyses and build fragility curves for the POE of certain inter-storey drift limits using the spectral acceleration at the fundamental period of the building as an intensity measure. Four different inter-storey drift limits were considered that are associated with different performance limit-states

applicable for light-frame wood structures. The limits of 1% and 2% were selected for Immediate Occupancy (IO) and Life Safety (LS) limit-states. These values are based on observation of damage of structural and non-structural components from shake-table tests of a full-scale 2-storey light-frame wood structure (Christovasilis et al., 2009a) and were also recommended in a study on the displacement-based design of this type of buildings (Pang et al., 2010). Two limits of 4% and 7% were considered for the Collapse Prevention (CP) perfomance level. The first value (4%) was adopted by Pang et al. (2010) while the second value (7%) was used in FEMA P695 (2009) as well as in a study on the collapse analysis of two light-frame wood buildings (Christovasilis et al., 2009b).

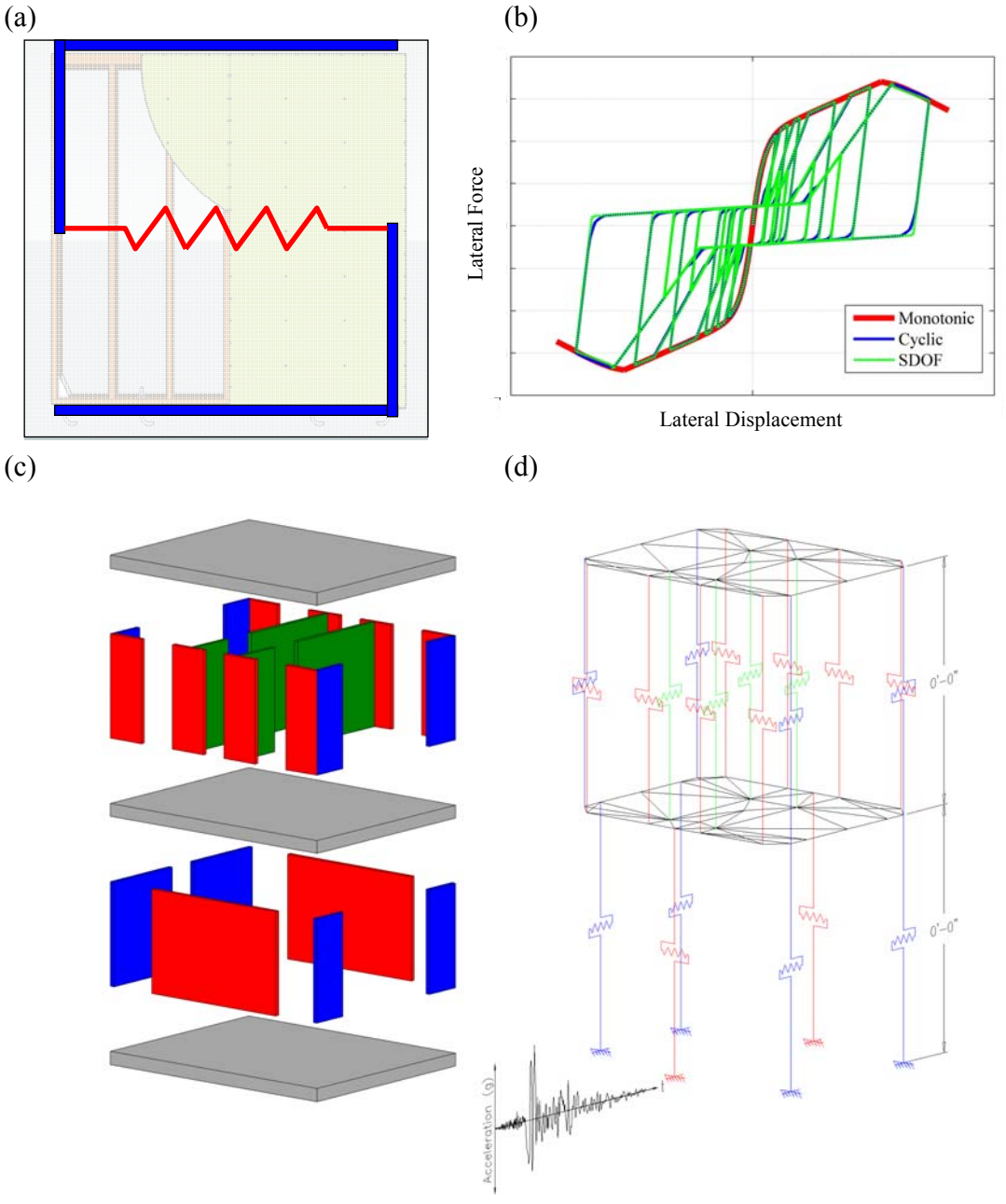

Figure 5. Modelling of light-frame wood buildings with CASHEW (Folz and Filiatrault 2001) and SAWS (Folz and Filiatrault 2004a, 2004b), (a) equivalent SDOF spring of a wood shear wall, (b) fitting of SDOF spring parameters to match the cyclic response of the wall assembly, (c) building sketch of a two-story light-frame wood structure, and (d) equivalent "pancake" building model (from Fischer *et al.* 2001)

The IDA results in terms of maximum inter-storey drift among all storeys of the building are shown in Figure 6. On the left (Figure 6a), the IDA curves result from the analyses with the different sets of motions defined within the proposed AMSA procedure. On the right (Figure 6a), the IDA curves are obtained from the analyses with the far-field record set of motions defined within FEMA P695. In this study (FEMA, 2009), a set of 22 pairs of ground motions were selected and normalized with different scale factors according to certain specifications. Then, the IDA is conducted by scaling with a global scale factor the normalized set of motions.

It is observed that the collapse of the structure occurs at higher values of spectral acceleration for the sets defined with AMSA procedure compared to the FEMA P695 set. However, the difference can only be quantified by building the fragility curves that relate the spectral acceleration at the fundamental period of the structure with the POE of the defined performance limit-states. These fragility curves are shown in Figure 7 for both cases and the values of mean μ and standard deviation β for each case are listed in Table 2.

These values were computed by applying a least squares fitting of a lognormal distribution on the numerical fragilities. The lognormally distributed fragility curve p for a given (μ, β) pair is given by (Eq. 1):

$$p = f(x \mid \mu,\beta) = \frac{1}{\sqrt{2\cdot\pi}\cdot\beta}\cdot\int_0^t \left(e^{\frac{-(\ln t-\mu)^2}{2\cdot\beta^2}} / t \right) dt \tag{1}$$

For each seismic intensity level, the numerical fragility curve was computed by counting the percentage of occurences P_j that a given limit is exceeded at each median spectral acceleration value α_j. The objective function minimized was then defined as given by (Eq. 2):

$$H = \sum_j \left[\left(P_j - f(x \mid \mu,\beta)\big|_{x=\alpha_j} \right)^2 \right] \tag{2}$$

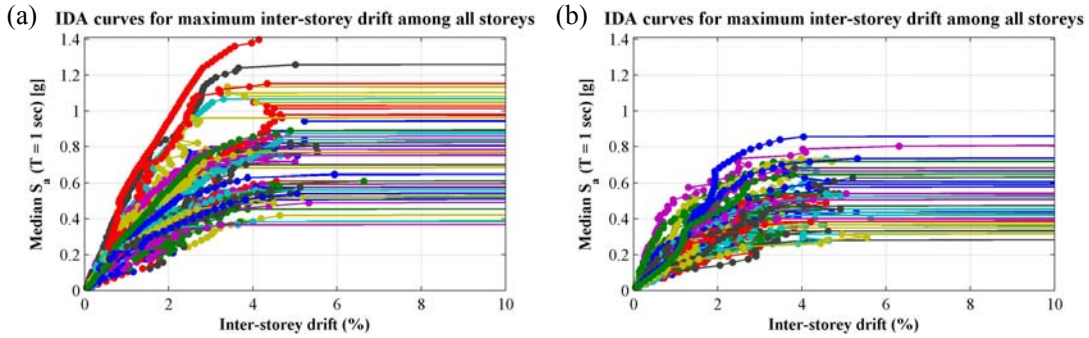

Figure 6. IDA curves for maximum inter-storey drift among all storeys: (a) for the sets of ground motions selected with the AMSA pocedure, and (b) for the FEMA P695 set of ground motions

Table 2. Mean and standard deviation of fragility curves for exceedence of certain limits of inter-storey drifts

	sets selected with the AMSA procedure		FEMA P695 set	
Inter-storey drift limit (%)	μ	β	μ	β
1	0.240	0.341	0.189	0.368
2	0.429	0.372	0.340	0.349
4	0.646	0.330	0.473	0.315
7	0.682	0.326	0.495	0.313

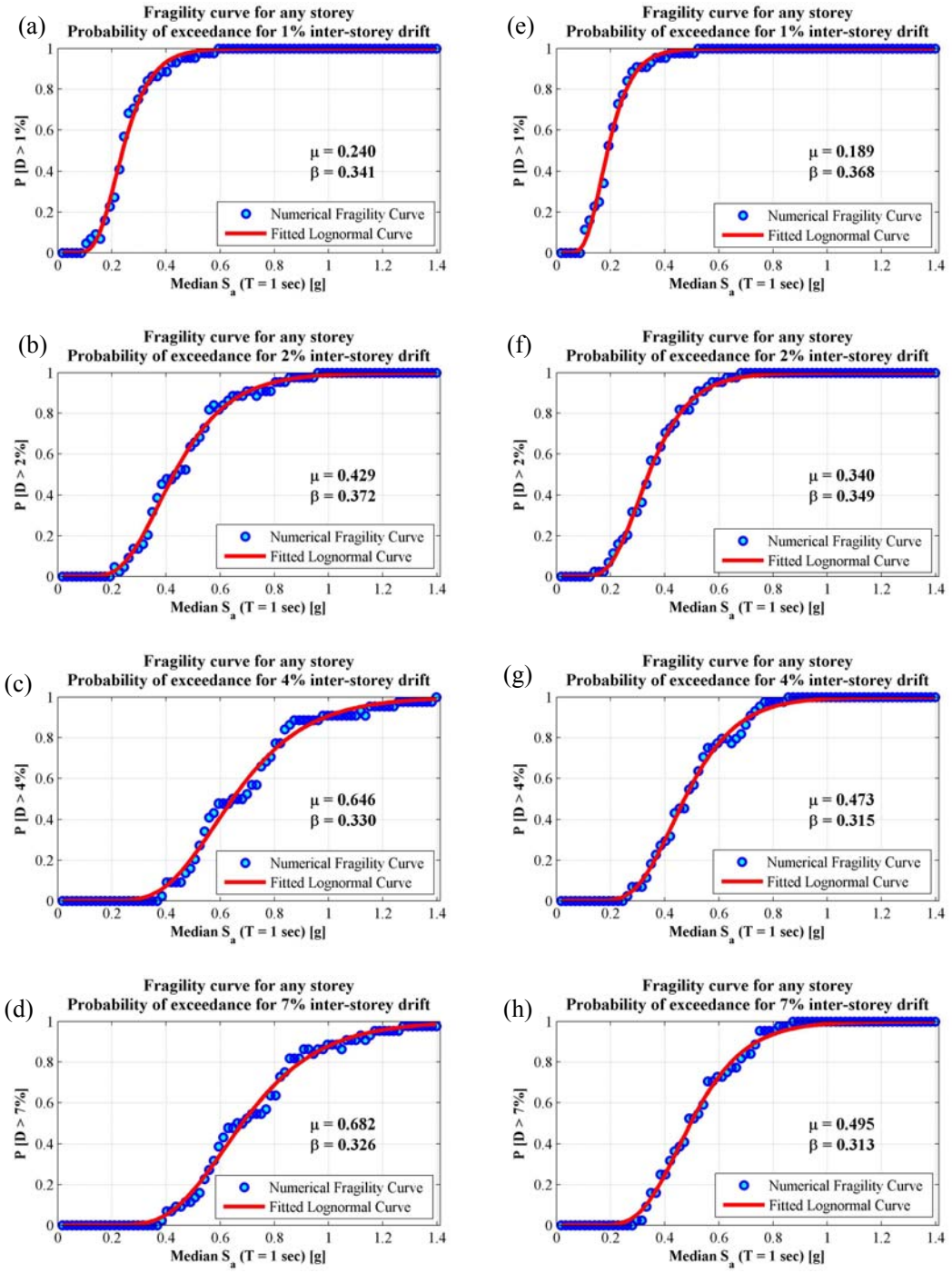

Figure 7. Numerical fragility curves and fitted lognormal distributions for exceedence of certain limits of inter-storey drifts: (a, b, c, d) for the sets of ground motions selected with the AMSA pocedure, and (e, f, g, h) for the FEMA P695 set of ground motions

Figure 8 summarizes the fragility curves for each case indicating with vertical lines the spectral acceleration corresponding to the 10% and 2% POE in 50 years. The fragilities obtained indicate that for this specific case-study the results obtained from the sets defined with the AMSA procedure are less conservative compared to the set of FEMA P695 since the mean values of spectral acceleration for the former case are consistently about 30% greater than those of the latter case. The standard deviation values are similar for both cases. The POE of the CP limit-states remains below 10% for both cases for

a shaking intensity of 2% POE in 50 years, which indicates that the seismic design of the building was successfully conducted

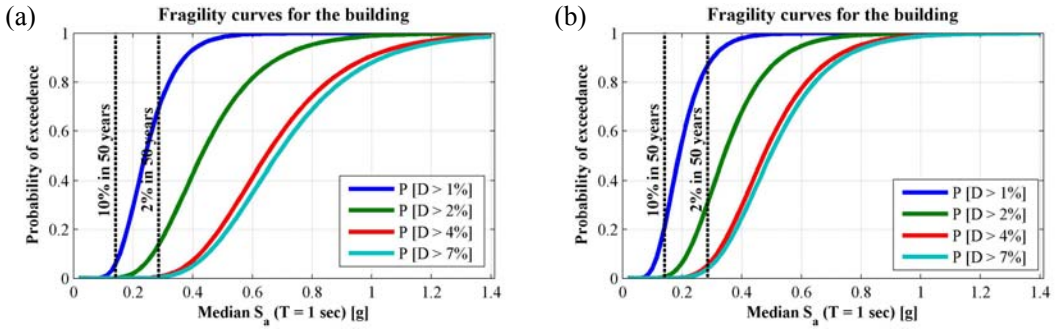

Figure 8. Summary of fragility curves for exceedence of certain limits of inter-storey drifts: (a) for the sets of ground motions selected with the AMSA procedure, and (b) for the FEMA P695 set of ground motions

CONCLUSIONS

This paper presents the effectiveness of the scaling method on the developing of fragility curves. Two datasets have been selected for comparison: (1) the dataset of FEMA P695 and (2) the *site specific dataset* developed using the proposed procedure. The structure considered for the application example is a 5-storey residential light-frame wood building. Results of the proposed scaling procedure are less conservative with respect to the set in FEMA P695, however more case studies are necessary to generalize this statement.

ACKNOWLEDGMENTS

The research leading to these results has received funding from the European Community's Seventh Framework Programme - Marie Curie International Reintegration Actions - FP7/2007-2013 under the Grant Agreement n° PIRG06-GA-2009-256316 of the project ICRED - Integrated European Disaster Community Resilience, and by the Marie Curie International Outgoing Fellowship (IOF) Actions-FP7/2007-2013 under the Grant Agreement n°PIOF-GA-2012-329871 of the project IRUSAT—Improving Resilience of Urban Societies through Advanced Technologies.

REFERENCES

Ambraseys N.N., Simpson K.A., Bommer J., (1996). Prediction of horizontal response spectra in Europe, Earthquake Engineering and Structural Dynamics, 25(4):371–400.

Baker, J.W., (2011). The conditional mean spectrum: A tool for ground motion selection, ASCE, Journal of Structural Engineering 137, 322–331.

Barani S., Spallarossa D., Bazzurro P., (2009). Disaggregation of Probabilistic Ground-Motion Hazard in Italy, Bulletin of the Seismological Society of America, 99:2638–2661.

Bradley, B. A. (2012). "A ground motion selection algorithm based on the generalized conditional intensity measure approach." Soil Dynamics and Earthquake Engineering, 40, 48-61.

Buratti, N., Stafford, P. J., and Bommer, J. J. (2011). "Earthquake Accelerogram Selection and Scaling Procedures for Estimating the Distribution of Drift Response." Journal of Structural Engineering, 137(3), 345-357.

Christovasilis, I.P., Filiatrault, A. and Wanitkorkul, A., (2009a). "Seismic Testing of a Full-Scale Two-Story Light-Frame Wood Building: NEESWood Benchmark Test," MCEER Technical Report 09-0005, Multidisciplinary Center for Earthquake Engineering, Buffalo, New York, 14260.

Christovasilis, I.P., Filiatrault, A., Wanitkorkul, A. and Constantinou, M.C., (2009b). "Incremental Dynamic Analysis of Woodframe Buildings", Journal of Earthquake Engineering and Structural Dynamics 38(4):477-496.

Cimellaro, G. P., Reinhorn, A. M., D'Ambrisi, A., and De_Stefano, M. (2011). "Fragility Analysis and Seismic Record Selection." Journal of Structural Engineering, ASCE, 137(3), 379-390.

Cimellaro, G.P., (2013). Correlation in spectral accelerations for earthquakes in Europe, Earthquake Engineering and Structural Dynamics, 42:623–633.

Corigliano, M., Lai, C. G., Rota, M., and Strobbia, C. L. (2012). "ASCONA: Automated Selection of COmpatible Natural Accelerograms." Earthquake Spectra, 28(3), 965-987.

Ergun, M., and Ates, S. (2013). "Selecting and scaling ground motion time histories according to Eurocode 8 and ASCE 7-05." Earthquakes and Structures, 5(2), 129-142.

FEMA P695, (2009). "Quantification of Building Seismic Performance Factors," Washington, D.C. : FEMA P695 Federal Emergency Management Agency.

Fischer, D., Filiatrault, A., Folz, B., Uang, C. M. and Seible, F., (2001). "Shake Table Tests of a Two-Story Woodframe House," CUREe Publication No. W-06, CUREE-Caltech Woodframe Project.

Folz, B. and Filiatrault, A., (2004a). "Seismic Analysis of Woodframe Structures. I: Model Formulation," Journal of Structural Engineering, ASCE, 130(9):1353-1360.

Folz, B. and Filiatrault, A., (2004b). "Seismic Analysis of Woodframe Structures. II: Model Implementation and Verification," Journal of Structural Engineering, ASCE, 130(9):1361-1370.

Folz, B., and Filiatrault, A., (2001). "Cyclic analysis of wood shear walls," ASCE, Journal of Structural Engineering, 127 (4), pp. 433-441.

Grigoriu, M. (2011). "To Scale or Not to Scale Seismic Ground-Acceleration Records." Journal of Engineering Mechanics, ASCE, 137(4), 284-293.

Haselton, C. B., Baker, J. W., Liel, A. B., and Deierlein, G. G. (2011). "Accounting for Ground-Motion Spectral Shape Characteristics in Structural Collapse Assessment through an Adjustment for Epsilon." Journal of Structural Engineering-Asce, 137(3), 332-344.

Heo, Y., Kunnath, S.K., and Abrahamson, N. (2011). Amplitude-scaled versus spectrum-matched seismic ground motions for seismic performance assessment. ASCE Journal of Structural Engineering, 137(3): 278–288. doi:10.1061/ (ASCE)ST.1943-541X.0000340.

I.N.G.V. (2013). "The National Institute of Geophysics and Vulcanology." http://www.ingv.it/en/.

Idriss I. M. and Seed H. B. (1968). Seismic Response of Horizontal Soil Layers. Journal of the Soil Mechanics and Foundations Division, ASCE, Vol. 94, No. 4, pp.1003-1031.

Jayaram, N., Lin, T., Baker, J.W., (2011). "A computationally efficient ground-motion selection algorithm for matching a target response spectrum mean and variance", Earthquake Spectra, 27(3):797-815.

Katsanos, E. I., and Sextos, A. G. (2013). "ISSARS: An integrated software environment for structure-specific earthquake ground motion selection." Advances in Engineering Software, 58, 70-85.

Kayhan, A. H. (2012). "Selection and Scaling of Ground Motion Records Using Harmony Search." Teknik Dergi, 23(1), 5751-5775.

Koboevic, S., Guilini-Charrette, K., Castonguay, P. X., and Tremblay, R. (2011). "Selection and scaling of NBCC 2005 compatible simulated ground motions for nonlinear seismic analysis of low-rise steel building structures." Canadian Journal of Civil Engineering, 38(12), 1391-1403.

Kottke, A., and Rathje, E. M. (2008). "A Semi-Automated Procedure for Selecting and Scaling Recorded Earthquake Motions for Dynamic Analysis." Earthquake Spectra, 24(4), 911-932.

Kunnath, S., and Ahmadi, A. (2013). "Selection of Ground Motions for Performance-Based Seismic Assessment of Structures." Advances in Civil Infrastructure Engineering, Pts 1 and 2, X. Y. Zhou and G. J. He, eds., 111-117.

Li, L., Wen, R., Zhou, B., and Shi, D. (2013). "Study on strong motion records database and selection methods." Advances in Civil Engineering Ii, Pts 1-4, X. D. Zhang, H. N. Li, X. T. Feng, and Z. H. Chen, eds., 2117-2121.

Luco, N., and Bazzurro, P. (2007). "Does amplitude scaling of ground motion records result in biased nonlinear structural drift responses?" Earthquake Engineering & Structural Dynamics, 36(13), 1813-1835.

Michaud, D., and Leger, P. (2014). "Ground motions selection and scaling for nonlinear dynamic analysis of structures located in Eastern North America." Canadian Journal of Civil Engineering, 41(3), 232-244.

Naeim, F., Alimoradi, A., and Pezeshk, S. (2004). "Selection and scaling of ground motion time histories for structural design using genetic algorithms." Earthquake Spectra, 20(2), 413-426.

NIST (National Institute of Standards and Technology). 2011. Selecting and scaling earthquake ground motions for performing response-time-history analyses. Report No. GCR 11-917-15, USA.

Pang, W., Rosowsky, D.V., Pei, S. and van de Lindt, J.W., (2010). "Simplified Direct Displacement Design of Six-Story Woodframe Building and Pretest Seismic Performance Assessment," Journal of Structural Engineering, ASCE, 136(7):813-825.

Shi, W., Pan, P., Ye, L., Xu, Y., and Wang, C. (2013). "Skyline-based ground motion selection method for nonlinear time history analysis of building structures." Earthquake Engineering & Structural Dynamics, 42(9), 1361-1373.

Spallarossa, D. and Barani, S., (2007). Disaggregazione della pericolosità sismica in termini di M-R-ε. Progetto DPC-INGV S1, Deliverable D14, http://esse1.mi.ingv.it/d14.html.

Vamvatsikos, D., and Cornell, C.A., (2002). "Incremental dynamic analysis", Earthquake Engineering & Structural Dynamics, 31(3), 491–514.